Secondary water pore formation for proton transport in a ClC exchanger revealed by an atomistic molecular dynamics simulation

Youn Jo Ko and Won Ho Jo*

Department of Materials Science and Engineering, Seoul National University, Seoul 151-742, Korea

Keywords: chloride conduction; ClC channel; ion channel; molecular dynamics simulation; proton conduction

* Corresponding author. Tel: +82-2-880-7192. Fax: +82-2-885-1748. Email address: whjpoly@ snu.ac.kr (W.H. Jo)

ABSTRACT

Several prokaryotic ClC proteins have been demonstrated to function as exchangers that transport both chloride ions and protons simultaneously in opposite directions. However, the path of the proton through the ClC exchanger and how the protein brings about the coupled movement of both ions are still unknown. In the present work, we demonstrate that a previously unknown secondary water pore is formed inside a ClC exchanger by using an atomistic molecular dynamics (MD) simulation. From the systematic simulations, it was determined that the glutamate residue exposed to the intracellular solution, E203, plays an important role as a trigger for the formation of the secondary water pore. Based on our simulation results, we conclude that protons in the ClC exchanger are conducted via a water network through the secondary water pore and we propose a new mechanism for the coupled transport of chloride ions and protons.

In the early 1980's, a protein from the electric organ of a *Torpedo* ray was found to be involved in the transport of chloride ions across the cell membrane[1,2]. Since this discovery, it has been widely accepted that this protein, identified as a member of the chloride channel (ClC) family, is simply a channel through which a chloride ion is conducted via electrostatic diffusion regulated by an ion gradient or voltage across the cell membrane. However, recent reports have shown that the several members of the ClC family are not channels, but instead are chloride ion/proton exchangers in which the flux of chloride ions is coupled to the flux of protons in the opposite direction with a stoichiometric ratio of 2:1[3-7]. Nevertheless, the pathway for proton conduction and the mechanism of coupled transport for chloride ions and protons have not been elucidated, although some studies have suggested clues for proton transport in the exchangers. Most notably, Accardi et al.[3,4] have proposed that the two

glutamate residues E148 and E203 of *Escherichia coli* (*E. Coli*) ClC exchanger, the former residue located adjacent to the extracellular side and the latter exposed to the intracellular solution, are involved in proton transport in ClC exchangers based on experimental results demonstrating that the coupled movement of protons and chloride ions vanishes when these residues are mutated. They have also proposed that the proton and chloride ion pathways are separate because the glutamate residue on the intracellular side (E203), which has been suggested to be involved in proton transport, is distant from the putative chloride ion pathway. To prove that these two pathways are separate, these researchers attempted to find a residue that could deliver a proton from E203 to E148[7]. Among many candidates, they focused on the highly conserved tyrosine residue Y445 because it has a hydroxyl side chain that lies halfway between the two glutamate residues E148 and E203. However, they found that the removal of the hydroxyl group from Y445 by mutating it to phenylalanine or tryptophan has no significant effect on the protein's electrophysiological behavior.

The primary objective of this study is to elucidate the proton pathway inside a ClC exchanger and to identify the role of E203 on the proton transport. For this purpose, we performed an atomistic molecular dynamics (MD) simulation, which has proven to be a useful tool to solve problems that cannot be addressed directly by laboratory experiments[8-10]. We used the crystallographic structure of the prokaryotic ClC protein from *E. coli*[11,12] as a model structure of a ClC exchanger for our simulations. Based on the results from atomistic MD simulation, a secondary pathway for proton transport was discovered and a mechanism for the coupled movement of chloride ions and protons is proposed.

RESULTS

Secondary water pore revealed by an atomistic simulation

According to the crystal structure of the ClC exchanger, water molecules are found at both extracellular and intracellular vestibules but not in the putative ion translocation pathway[11,12]. Under these circumstances, it is hypothesized that a proton is not able to pass through the pathway due to the absence of a continuous water network that is a prerequisite for proton conduction. Although the mechanism of proton transport in a ClC exchanger has not been elucidated, recent result[4] has shown that proton transport in a prokaryotic ClC exchanger is impaired when E203 is mutated to a glutamine that functions to mimic the protonated state of a glutamate residue.

Inspired by these results, we performed MD simulations by varying the protonation state of E203 to confirm the structural change caused by the protonation state of E203. Here, the glutamate residue adjacent to the extracellular side, E148, which is known to be a key residue for chloride ion conduction, was kept protonated. Figure 1a shows the equilibrated structure of the ClC exchanger with the pore, as predicted by the HOLE program[13], where E203 is deprotonated and two chloride ions are bound to the positions resolved by X-ray crystallography (S_{int} and S_{cen}). Here, the predicted pore is consistent with the chloride ion pathway, and a water molecule was not observed inside the pore during the equilibration, as previously reported[11,12,14]. However, as E203 is protonated and the two chloride ions inside the chloride ion pathway are transported to the outside of the pore, a significant structural change occurs. After 2 ns equilibration, the region between the Y445 and E203 residues is rapidly filled with water molecules originating from the intracellular side, as shown in Figure 1b. Consequently, the water molecules form a continuous network that links E203 with E148; a previously unknown region that is predicted to be a pore by the HOLE program. Initially, we assumed this network of water molecules was an intermediate and expected that the water pore would disappear as the system reached equilibrium. However, this water pore was continued for an additional 12 ns (supplementary Video 1 online). Hence, we refer to this

novel water pore as ‘the secondary pore’, whereas the chloride ion pathway previously determined by X-ray crystallography is referred to as ‘the primary pore’.

Role of E203 as a gate

To investigate the reason of the formation of the secondary pore, the structural change caused by protonation of E203 was investigated in detail by overlapping the two structures shown in Figure 1a and b. As shown in Figure 1c, the most notable change in the protein structure was found near E203. Before protonation, the negatively charged side chain of E203 interacts with the positively charged arginine residue (R28) of another subunit of the protein via charge-charge interactions. However, when E203 lost its negative charge by protonation, the charge-charge interaction between E203 and the R28 was broken. In such a case, R28 is separated from E203, which results in the formation of a cleft between E203 and R28. Water molecules penetrated into the secondary pore through this cleft, and a continuous water network was formed inside the secondary pore, as shown in Figure 1b. It seems that E203 acts as a gate that triggers the formation of the secondary water pore through the breakage of charge-charge interaction with R28, an observation that is reminiscent of E148 acting as a gate for chloride ion conduction by the charge-dipole interaction with α-helix N[12]. The role of E203 as a gate became more evident when we compared the distance between deprotonated E203 and R28 with that between protonated E203 and R28. As shown in Figure 2, the distance between E203 and R28 remained nearly unchanged at approximately 2Å before protonation. However, these residues moved apart from each other as E203 lost its charge by protonation. Thus, it is clear that the protonation of E203 is a prerequisite for the formation of the secondary pore.

It is also possible that there are several other factors that may be involved in the formation of the secondary pore. To investigate whether other factors are necessary for the secondary

pore formation, we systematically generated structures with an embedded ClC exchanger by varying the position of the chloride ion and the protonation state of the E148 and E203 residues. As summarized in Table 1, the secondary pore was formed only when both E148 and E203 were protonated and the chloride ions at the primary pore were moved to outside of the pore, which implies that the formation of the secondary pore is affected not only by the protonation state of E148 and E203, but also by the position of the chloride ion inside the primary pore. Here, it is interesting to note that the secondary pore was always filled with water molecules originating from the intracellular side whereas no water molecules were observed to migrate from the extracellular side.

Proton transport via the secondary water pore

Based on the result that the formation of the continuous water network inside the secondary pore is dependent on the protonation state of E203 that is known to be involved with proton transport[4], it is reasonable to assume that this water pore is a pathway for proton transport because a proton is easily transported along the continuous water network by hop-and-turn, or the "Grotthuss mechanism"[15]. According to experimental results[3,4], the ClC exchanger loses its ability to transport protons when E203 is mutated to a glutamine (E203Q). Thus, a secondary water pore that transports protons should not be formed in the mutant E203Q ClC exchanger if our assumption is correct. To determine whether the secondary water pore is formed in the mutant ClC exchanger (E203Q), a ClC exchanger in which E203 is mutated to glutamine was equilibrated for 14 ns using MD simulation. In the mutated structure, it was observed that the E203Q interacted with R28 via hydrogen bonding (Fig. 3a). We also noted that the hydrogen bonding between E203Q and R28 prevented water molecules on the intracellular side from entering into the secondary pore, as did the charge-charge interaction between E203 and R28 in the wild type (see Fig. 1a and 3a). Nonetheless, these two

structures (wild vs. mutated) have a significant difference in the way of controlling the interaction between E203 (Q203 in the mutant exchanger) and R28. In contrast to the wild type ClC exchanger, which is able to control the interaction between E203 and R28 by gaining or losing a negative charge based on the protonation state of E203, the E203Q ClC exchanger kept interacting with R28 irrespective of the protonation state of Q203. As a result, the formation of the secondary pore was not observed in the mutant exchanger (E203Q), as summarized in Table 1. This result explains why the mutated ClC exchanger lost its function of proton transport when E203 was mutated to glutamine. Based on these results, it can be concluded that the secondary pore is a pathway for proton transport in ClC exchangers.

These results are consistent with another hypothesis that suggesting the proton pathway is separate from the chloride ion pathway and that the two pathways are bifurcated at E148 toward the intracellular side[3,4]. However, this hypothesis assumed that protons would be transported through this pathway via a protein residue[7], rather than a continuous water network, which highlights the following unresolved issues: First, proton movement along the protein's residues must be coupled to the occupancy of the binding sites of chloride ions. Second, the distance between E148 and E203 is farther than 15Å, which is too far of a distance for a proton to cross in a single hop. Assuming that the secondary water pore discovered in this work is a proton pathway, these issues are easily explained: First, proton conduction in a ClC exchanger is coupled to chloride ion transport because the secondary pore is formed only when the chloride ions inside the chloride ion pathway are moved to the outside of the pore. Second, a proton can be easily transported between E203 and E148 along the continuous water network by hop-and-turn, or the "Grotthuss mechanism"[15].

Role of Y445 as a barrier between the proton and chloride ion pathway

For a proton to be transported from E203 to E148, a series of protein residues or a continuous water network that can mediate the proton movement is required. Accardi et al.[7] focused on the highly conserved tyrosine residue Y445 as a candidate for proton transport because it is the only residue that has a hydroxyl side group that lies halfway between E203 and E148. However, they found that mutation of Y445 to phenylalanine (F) or tryptophan (W) has no significant effect on the electrophysiological behavior of the exchanger. Here, it is noteworthy that the aromatic side group of Y445 is similar to that of phenylalanine and tryptophan except hydroxyl group.

To determine the role of the Y445 hydroxyl group in proton transport, a ClC exchanger in which the tyrosine residue was mutated to a phenylalanine (Y445F) was generated for MD simulations. As shown in Table 1 and Figure 3b, the secondary pore was formed in the structure containing Y445F as in the wild type structure. In addition, no differences were observed in how the aromatic side chain of both Y445 and Y445F separated the secondary pore from the chloride ion pathway. When the chloride ions inside the primary pore were transported to the outside of the pore, the side chain of the tyrosine residue was rotated slightly toward the primary pore, which resulted in the expansion of the secondary water pore, as shown in Figure 1b and c. It is known that the primary role of the tyrosine residue is to stabilize a chloride ion through the hydroxyl group when the ion is bound at the S_{cen} position[11,12]. In addition to its primary role, it seems that the tyrosine residue may have a secondary role where it functions as a barrier that separates the secondary pore from the primary pore via the aromatic side group. Based on these assumptions, the removal of the hydroxyl group from the tyrosine residue should not affect the formation of the secondary water pore. This hypothesis is supported by the experimental results demonstrating that proton transport was not impaired by the removal of the hydroxyl group from the tyrosine residue by the mutations Y445F and Y445W[7].

CONCLUSIONS

In the present work, a secondary water pore in a ClC exchanger was revealed using atomistic MD simulation. The secondary water pore is formed between the intracellular residue E203 and the extracellular residue E148. The systematic research revealed that the secondary water pore is formed only when both E148 and E203 are protonated and the chloride ions inside the chloride ion pathway are transported to the outside. It was also determined that E203 interacts with R28 and functions as a gate that controls the formation of the secondary pore by losing or gaining a negative charge according to its protonation state. In addition, Y445 was demonstrated to function as a barrier that separates the secondary water pore from the chloride ion pathway. We conclude that the secondary pore is a pathway for proton conduction on the basis of the following results: First, the secondary pore is formed only when E203, which is known to be a key residue for proton transport[3,4], loses its charge by protonation. Second, a continuous water network inside the secondary pore links E203 and E148, two residues known to be involved in the proton transport in ClC exchangers. Third, assuming the secondary water pore is a proton pathway, two unresolved issues introduced by the previous proposal[4] are now resolved. Fourth, the highly conserved Y445 functions as a barrier that separates the secondary pore from the chloride ion pathway, supported by the experimental result[7] that removal of the hydroxyl group from Y445 does not affect the electrophysiological behavior of the exchanger. Finally, considering that the secondary water pore for proton conduction is formed when two chloride ions inside the chloride ion pathway are transported to the outside of the pore, it is clear why the flux of chloride ions is coupled to the flux of protons in the opposite direction with a stoichiometric ratio of 2:1. In light of these results, we hypothesize that the transport of chloride ions in a ClC exchanger is coupled to proton transport as illustrated in Figure 4. First, the protonation of E148 causes the primary

pore to be opened, which results in chloride ion conduction (Fig. 4a). After the chloride ions pass through the primary pore, the interaction between E203 and the R28 is broken, resulting in the formation of a water network in the secondary pore (Fig. 4b). Next, the proton belonging to protonated E148 is transferred to a water molecule inside the secondary pore, and subsequently the primary pore is closed by deprotonation of E128 (Fig. 4c). Finally, the proton is able to pass through the secondary pore via the water network (Fig. 4d).

Although this work demonstrates that ClC exchangers conduct protons via the water network formed inside the secondary pore rather than by a protein residue, it still remains to be elucidated why the simultaneous protonation of E203 and E148 is required for the secondary pore formation. Also, additional experimental and theoretical investigations are required to verify that a proton can be transported via this water network. Nonetheless, we believe that the discovery of the secondary water pore in a ClC exchanger is a stepping stone to better understand the unique characteristics of ClC exchangers in which chloride ion transport is coupled to proton transport and a good example for prediction *in silico* precedent of verification *in vivo*.

METHODS

Structural simulations were performed using the wild type ClC crystal structure, Protein Data Bank (PDB) code 1OTS, which has recently been resolved by X-ray crystallography at 2.5Å resolution from *Escherichia coli*[12]. The two chloride ions at positions S_{int} and S_{cen} in the crystal were preserved. The positions S_{int} and S_{cen} were designated according the notation of Dutzler et al.[12] The initial structure was embedded in a 16:0-palmytoyl,18:1(Δ^9)-oleoylphosphatidylethanolamine lipid bilayer, which is generally accepted as a good model for the *E. coli* membrane[16]. The lipid bilayer with the embedded ClC protein was hydrated with approximately 30 Å thick water layers. The final structure contained approximately

87,600 atoms and was energy-minimized by the conjugated gradient method. First, only water molecules were minimized while the other atoms were fixed with constraints; the constraints imposed on the lipid molecules and the protein were then sequentially released so that the ClC protein became free to move. The generated membrane structure was equilibrated using MD simulation for 4 ns with an NPT ensemble. To elucidate the role of E148 and E203 in proton transport, different initial structures were generated by modifying the protonation state of E148 and E203, as well as the position of the chloride ions. In addition, the role of the hydroxyl group of Y445 was investigated by mutation to a phenylalanine. The structure with E203 mutated to a glutamine (E203Q) was also generated to confirm previous experimental results[4]. Each modified structure, summarized in Table 1, was equilibrated for 14 ns, and the structural changes caused by the modification are observed. The Langevin piston algorithm was used for constant pressure and temperature. Pressure and temperature were set to 1 atm and 310 K, respectively. The particle mesh Ewald (PME) summation was used for the calculation of the electrostatic force without cutoff[17]. The electrostatic neutralization of the system, which is a prerequisite for PME, was satisfied by adding an appropriate number of sodium and chloride ions to each modified structure. All calculations were performed using the NAMD program for parallel computation[18]. The CHARMM force field with all-atom parameters was used: CHARMM22 for protein[19], CHARMM27 for phospholipids[20], and the TIP3P model for water molecules[21]. For sodium and chloride ions[22], parameters in the CHARMM force field were used without modification. The HOLE program[13], which has been widely used for the prediction of the pore in channel proteins, is used for the pore analysis. All simulations were performed on our local Linux cluster.

ACKNOWLEDGEMENTS

The authors acknowledge the Ministry of Science and Technology, Korea for financial support of this work through the Global Research Laboratory (GRL) program.

REFERENCES

1. Miller, C. Open-state substructure of single chloride channels from *Torpedo* electroplax. *Phil. Trans. R. Soc. B.* **299**, 401-411 (1982).

2. Miller, C. & White, M.M. Dimeric structure of single chloride channels from Torpedo Electroplax. *Proc. Natl. Acad. Sci.* **81**, 2772-2775 (1984).

3. Accardi, A. & Miller, C. Secondary active transport mediated by a prokaryotic homologue of ClC Cl^- channels. *Nature.* **427**, 803-807 (2004).

4. Accardi, A., Walden, M., Nguitragool, W., Jayaram, H., Williams, C. & Miller, C. Separate ion pathways in a Cl^-/H^+ exchanger. *J. Gen. Physiol*. **126**, 563-570 (2005).

5. Picollo, A. & Pusch, M. Chloride/proton antiporter activity of mammalian CLC proteins ClC-4 and ClC-5. *Nature.* **436**, 420-423 (2005).

6. Scheel, O., Zdebik, A.A., Lourdel, S. & Jentsch, T.J. Voltage-dependent electrogenic chloride/proton exchange by endosomal CLC proteins. *Nature.* **436**, 424-427 (2005).

7. Accardi, A., Lobet, S., Williams, C., Miller, C. & Dutzler, R. Synergism between halide binding and proton transport in a CLC-type exchanger. *J. Mol. Biol.* **362**, 691-699 (2006).

8. Choi, H.S., Huh, J. & Jo, W.H. Electrostatic energy calculation on the pH-induced conformational change of influenza virus hemagglutinin. *Biophys. J.* **91**, 55-60 (2006).

9. Choi, H.S., Huh, J. & Jo, W.H. pH-induced helix-coil transition of amphipathic polypeptide and its association with the lipid bilayer: Electrostatic energy calculation. *Biomacromolecules* **7**, 403-406 (2006).

10. Ko, Y.J., Huh, J. & Jo, W.H. Ion exclusion mechanism in aquaporin at an atomistic level. *Proteins* **70**, 1442-1450 (2008).

11. Dutzler, R., Campbell, E.B., Cadene, M., Chait, B.T. & MacKinnon, R. X-ray structure of a CIC chloride channel at 3.0 Å reveals the molecular basis of anion selectivity. *Nature* **415**, 287-294 (2002).

12. Dutzler, R., Campbell, E.B. & MacKinnon, R. Gating the selectivity filter in ClC chloride channels. *Science* **300**, 108-112 (2003).

13. Smart, O.S., Goodfellow, J.M. & Wallace, B.A. The pore dimensions of gramicidin-A. *Biophys. J.* **65**, 2455-2460 (1993).

14. Dutzler, R. Structural basis for ion conduction and gating in ClC chloride channels. *Febs Lett.* **564**, 229-233 (2004).

15. Agmon, N. The Grotthuss Mechanism. *Chem. Phys. Lett.* **244**, 456-462 (1995).

16. Tieleman, D.P. & Berendsen, H.J.C. A molecular dynamics study of the pores formed by Escherichia coli OmpF porin in a fully hydrated palmitoyloleoylphosphatidylcholine bilayer. *Biophys. J.* **74**, 2786-2801 (1998).

17. Darden, T., York, D. & Pedersen, L. Particle mesh Ewald: An *N*·Log(*N*) method for Ewald sums in large systems. *J. Chem. Phys.* **98**, 10089-10092 (1993).

18. Phillips, J.C. et al. Scalable molecular dynamics with NAMD. *J. Comput. Chem.* **26**, 1781-1802 (2005).

19. MacKerell, A.D. et al. All-atom empirical potential for molecular modeling and dynamics studies of proteins. *J. Phys. Chem. B* **102**, 3586-3616 (1998).

20. Merz, K.M. & Roux, B. *Biological membranes : a molecular perspective from computation and experiment*, xiii, 593 p. (Birkhauser, Boston, 1996).

21. Jorgensen, W.L., Chandrasekhar, J., Madura, J.D., Impey, R.W. & Klein, M.L. Comparison of simple potential functions for simulating liquid water. *J. Chem. Phys.* **79**, 926-935 (1983).

22. Beglov, D. & Roux, B. Finite Representation of an infinite bulk system - solvent boundary potential for computer-simulations. *J. Chem. Phys.* **100**, 9050-9063 (1994).

FIGURE LEGENDS

Figure 1. Structural representations of *E. coli* ClC exchanger. Equilibrated structures of the ClC exchanger with the primary pore (a) and the secondary pore (b) are shown and two structures overlapped are shown in (c) to compare the structural differences between (a) and (b). Two chloride ions are represented as green spheres in (a) and the pores predicted by the HOLE program are shown with yellow transparent color in (a) and (b). The structures (a) and (b) are colored red and blue in (c), respectively. D, F, and N helices are shown by cartoon representation and key residues are shown in stick representation. All the snapshot figures in this paper are created with PyMOL (www.pymol.org).

Figure 2. Distance between E203 and R28 during the equilibration simulation. Blue and red lines represent the distances when E203 is protonated and deprotonated, respectively.

Figure 3. Structural representations of *E. coli* mutant ClC exchangers. Simulations were performed with mutants E203Q (a) and Y445F (b). D, F, and N helices are shown by cartoon representation and key residues are shown in stick representation. Hydrogen bonding between Q203 and R28 is represented with red lines.

Figure 4. Schematic representation of the coupled movement of chloride ions and protons through the primary and secondary pores of the ClC exchanger. Helices D, F, and N are represented by grey cylinders. Chloride ions (a) are represented as green spheres and protons are represented as yellow spheres. (a) Protonation of E148 causes the primary pore to be opened, which results in chloride ion conduction. (b) After the chloride ions pass through the primary pore, the interaction between E203 and the R28 is broken due to the protonation of E203, resulting in the formation of a water network in the secondary pore. (c) A proton belonging to E128 is transferred to a water molecule in the secondary pore and passes through the secondary pore via the water network.

	Conditions used in simulation			the formation of the secondary pore
	protonation of E203	protonation of E148	number of Cl^- at the primary pore	
WT	O	O	2	X
			0	O
		X	2	X
			0	X
	X	O	2	X
			0	X
		X	2	X
			0	X
Y445F	O	O	0	O
		X	0	X
E203Q	E → Q	O	0	X
		X	0	X

Table 1. Atomistic molecular dynamics simulation conditions for the ClC exchanger from *Escherichia coli*. The configuration for each structure simulation was equilibrated for 14 ns. The inclusion of a simulation condition (protonation of E203 or E148) or the formation of the secondary pore is denoted by (O) and the exclusion of a simulation condition (protonation of E203 or E148) is denoted by (X).

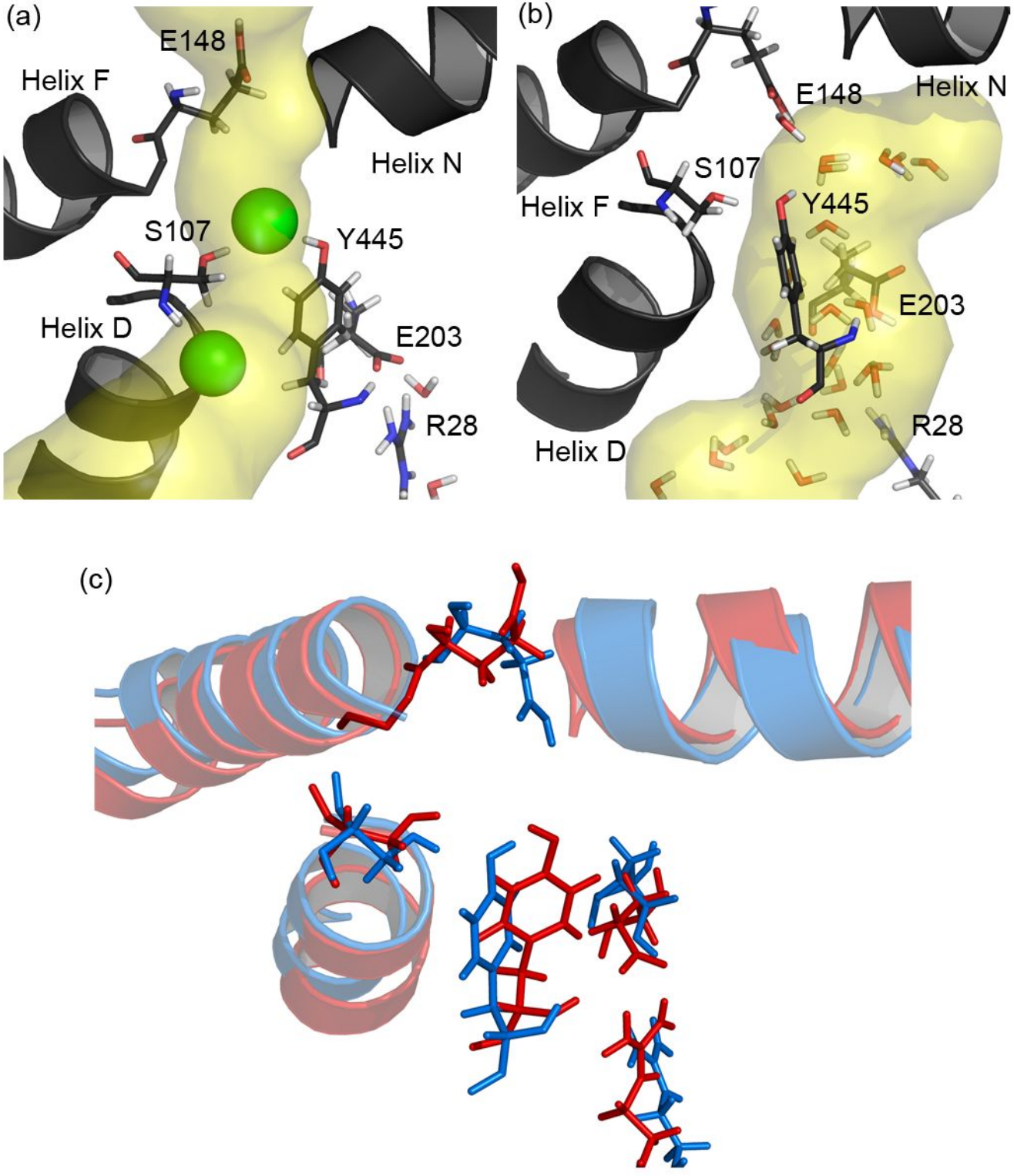
(a)
E148
Helix F
Helix N
S107
Y445
Helix D
E203
R28
(b)
E148
Helix N
S107
Helix F
Y445
E203
R28
Helix D
(c)

Figure 1

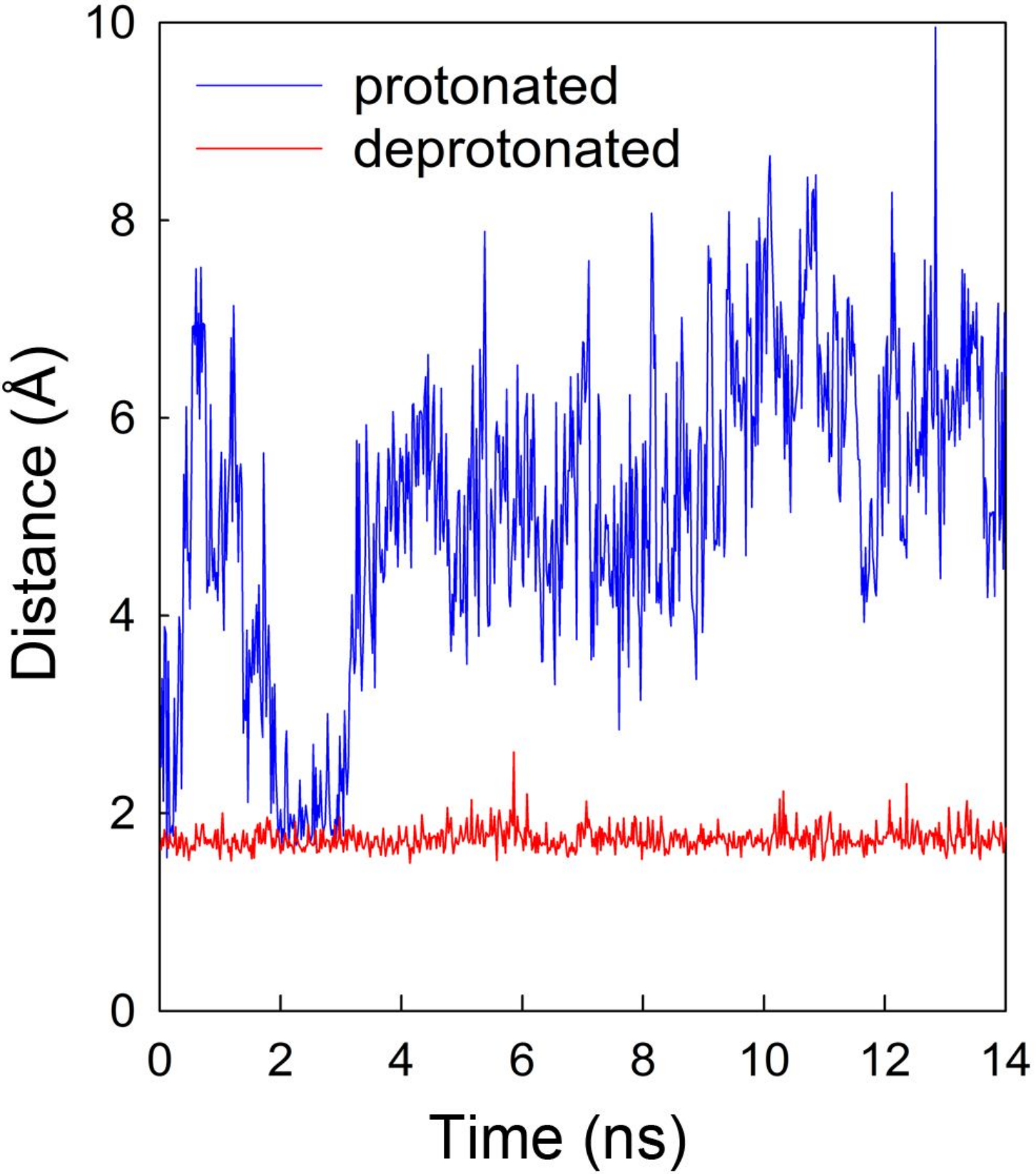

Figure 2

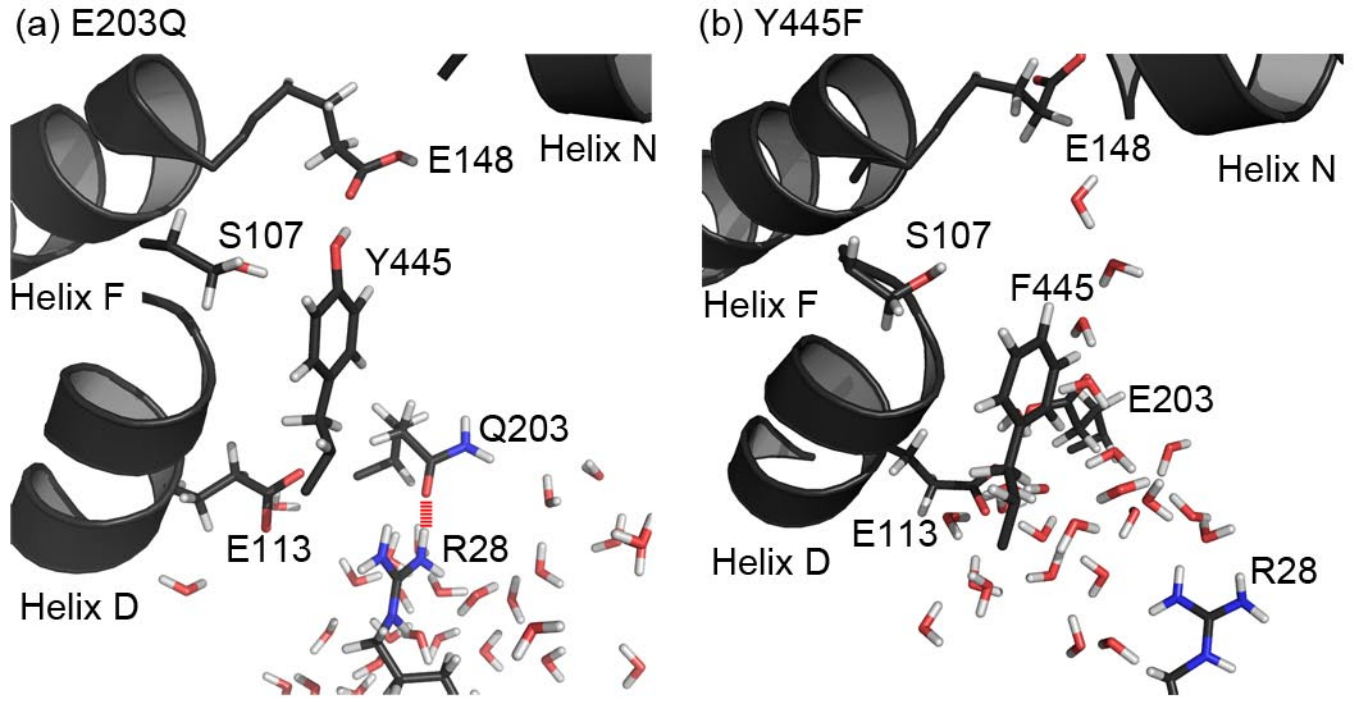
(a) E203Q
E148
Helix N
S107
Y445
Helix F
Q203
E113
R28
Helix D
(b) Y445F
E148
Helix N
S107
F445
Helix F
E203
E113
Helix D
R28

Figure 3

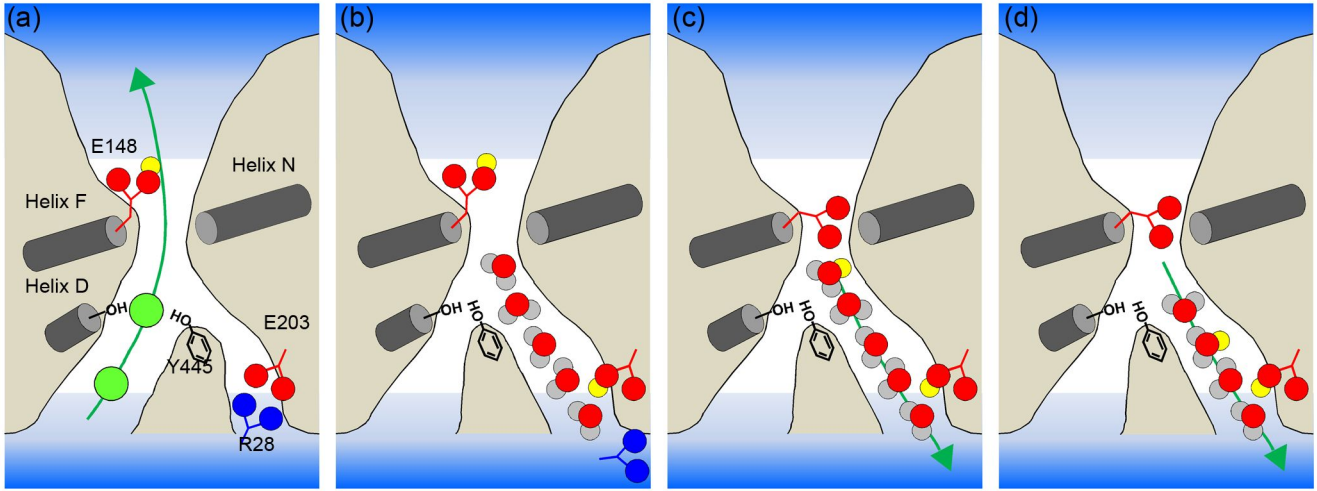
(a)
E148
Helix N
Helix F
Helix D
OH
HO
E203
Y445
R28
(b)
OH
HO
(c)
OH
HO
(d)
OH
HO

Figure 4